# Statins Reduce Intratumor Cholesterol Affecting Adrenocortical Cancer Growth

Francesca Trotta[1], Paola Avena[1], Adele Chimento[1], Vittoria Rago[1], Arianna De Luca[1], Sara Sculco[1], Marta C. Nocito[1], Rocco Malivindi[1], Francesco Fallo[2], Raffaele Pezzani[2], Catia Pilon[2], Francesco M. Lasorsa[3], Simona N. Barile[3], Luigi Palmieri[3], Antonio M. Lerario[4], Vincenzo Pezzi[1], Ivan Casaburi[1], and Rosa Sirianni[1]

## ABSTRACT

Mitotane causes hypercholesterolemia in patients with adrenocortical carcinoma (ACC). We suppose that cholesterol increases within the tumor and can be used to activate proliferative pathways. In this study, we used statins to decrease intratumor cholesterol and investigated the effects on ACC growth related to estrogen receptor α (ERα) action at the nuclear and mitochondrial levels. We first used microarray to investigate mitotane effect on genes involved in cholesterol homeostasis and evaluated their relationship with patients' survival in ACC TCGA. We then blocked cholesterol synthesis with simvastatin and determined the effects on H295R cell proliferation, estradiol production, and ERα activity *in vitro* and in xenograft tumors. We found that mitotane increases intratumor cholesterol content and expression of genes involved in cholesterol homeostasis, among them *INSIG*, whose expression affects patients' survival. Treatment of H295R cells with simvastatin to block cholesterol synthesis decreased cellular cholesterol content, and this affected cell viability. Simvastatin reduced estradiol production and decreased nuclear and mitochondrial ERα function. A mitochondrial target of ERα, the respiratory complex IV (COXIV), was reduced after simvastatin treatment, which profoundly affected mitochondrial respiration activating apoptosis. Additionally, simvastatin reduced tumor volume and weight of grafted H295R cells, intratumor cholesterol content, Ki-67 and ERα, COXIV expression and activity and increase terminal deoxynucleotidyl transferase dUTP nick end labeling–positive cells. Collectively, these data demonstrate that a reduction in intratumor cholesterol content prevents estradiol production and inhibits mitochondrial respiratory chain–inducing apoptosis in ACC cells. Inhibition of mitochondrial respiration by simvastatin represents a novel strategy to counteract ACC growth.

## Introduction

Adrenocortical carcinoma (ACC) is a rare but aggressive cancer with a very poor prognosis. At present, the only valuable option for ACC therapy is an early prognosis followed by surgical resection of the tumor. Mitotane (1,1-dichloro-2-(ochlorophenyl)-2-(p-chlorophenyl)-ethane or o,p-DDD), an inhibitor of steroid synthesis with adrenolytic activity, alone or combined with cytotoxic drugs such as etoposide, doxorubicin, and platinum agents, is the only specific treatment for ACC (1). Overall survival rate at 5 years is 16% to 38%, but in the case of metastatic disease (stage IV), survival rate at 5 years drops to less than 10% (2). Because mitotane treatment has a relatively low response rate and carries significant systemic toxicity, better treatment methods are critically needed for more effective targeting and inhibition of ACC.

Mitotane works by inhibiting cytochrome P450s involved in steroid synthesis and by inhibiting SOAT1, an enzyme involved in cholesterol esterification, leading to an increase in free cholesterol toxic to the cell. Mitotane serum concentrations above 14 mg/L are required for its therapeutic effects (3). However, even with administration of high doses, effective mitotane serum concentrations are achieved in only half of patients and are never reached in others (4). Doses below 14 mg/L are less effective in inhibiting SOAT1, but still able to induce 3-hydroxy-3-methylglutaryl-coenzyme A reductase (HMGCR) activity in the liver (5), favoring an increase in serum cholesterol levels, a side effect that patients with ACC experience during mitotane treatment (6). Possibly, the increase in serum cholesterol will allow the adrenal tumor to have a higher uptake. Alternatively, a direct effect of mitotane on adrenal HMGCR, affecting *de novo* synthesis, cannot be excluded, because the adrenal can synthesize cholesterol in the endoplasmic reticulum (7). Both uptake or *de novo* synthesis will increase cholesterol availability within the tumor cells, favoring activation of proliferative mechanisms.

Our previous studies have demonstrated that ACC is characterized by aromatase overexpression (8), and insulin-like growth factor II (resulting overexpressed in 90% of ACCs and activating an autocrine mitogenic effect) can induce aromatase transcription (9). Then, it is possible that in patients with ACC, despite normal circulating estrogen levels, a higher local estrogen production can occur, allowing estrogens, through estrogen receptor α (ERα), to foster ACC progression.

[1]Department of Pharmacy, Health and Nutritional Sciences, University of Calabria, Arcavacata di Rende, Cosenza, Italy. [2]Department of Medical and Surgical Sciences, University of Padua, Padua, Italy. [3]Department of Biosciences, Biotechnologies and Biopharmaceutics, University of Bari, and CNR Institute of Biomembranes, Bioenergetics and Molecular Biotechnologies, Bari, Italy. [4]Departments of Molecular and Integrative Physiology and Internal Medicine, University of Michigan, Medical School, Ann Arbor, Michigan.

**Note:** Supplementary data for this article are available at Molecular Cancer Therapeutics Online (http://mct.aacrjournals.org/).

F. Trotta, P. Avena, and A. Chimento contributed equally to this article.

I. Casaburi and R. Sirianni contributed equally as the co-senior authors of this article.

**Corresponding Authors:** Rosa Sirianni, University of Calabria, Edificio Polifunzionale, Arcavacata di Rende (CS), Cosenza 87036, Italy. Phone: 39-0984-493182; Fax: 39-0984-493157; E-mail: rosa.sirianni@unical.it and Vincenzo Pezzi, Phone: 39-0984-493148; Fax: 39-0984-493157; E-mail: v.pezzi@unical.it

Mol Cancer Ther 2020;19:1909–21

**doi:** 10.1158/1535-7163.MCT-19-1063

A study performed on 152 patients with ACC showed that increased intra-abdominal fat is associated with tumor worsening and decreased survival (10). The rise in fat deposition observed in mitotane-treated patients can also be responsible for increased estradiol production, because the adipose tissue has high aromatase expression, which can convert steroid precursors into estrogens (11). Importantly, it has been recently suggested that adipose tissue may contain the steroidogenic machinery necessary for the initiation of *de novo* steroid biosynthesis from cholesterol (12). The increase in cholesterol and body fat is also responsible for lowering hematic mitotane concentration, because the drug is a lipophilic compound and accumulates into circulating lipoprotein fractions and high-lipid–containing tissues (13).

A drug capable of reducing cholesterol synthesis both at hepatic and intratumor levels would be effective in preventing ACC growth. In this study, we propose statins, drugs that target HMGCR, largely used to reduce hypercholesterolemia as a valid treatment for ACC. By reducing cholesterol synthesis within the tumor cells, statins could be a reliable mean to prevent estrogen production and then action through ERα in ACC.

## Materials and Methods

Detailed experimental information is provided in the Supplementary Experimental Procedures.

### Cell cultures and tissue

H295R, SW13, and Y1 cells were purchased from the ATCC. H295R cells were cultured as previously described (14). SW13 cells were maintained in DMEM/F-12 with 10% FBS. Y1 cells were maintained in DMEM/F-12 with 2.5% FBS and 15% horse serum. Cell monolayers were subcultured into 6-well plates for protein and RNA extraction ($4 \times 10^6$ cells/plate) and 12 multiwell for colony formation assay ($1 \times 10^3$ cells/well) and grown for 14 days. Cells were treated with statins or mitotane (Sigma) in DMEM/F-12 containing 10% FBS.

Fresh-frozen samples of adrenocortical tumors, removed at surgery, were collected at the hospital-based Divisions of the University of Padua (Italy). Tissue samples were obtained with the approval of local ethics committees and written-informed consent from patients. Studies were conducted in accordance with the Declaration of Helsinki guidelines as revised in 1983 and approved by the institutional review board of the University of Padua. Diagnosis of malignancy was performed according to the histopathologic criteria proposed by Weiss and colleagues (15) and the modification proposed by Aubert and colleagues (16). Patients included in the mitotane-treated group received the drug for at least 4 months at the dose of 4 to 6 g/day.

### MTT assay

The effect of simvastatin on cell viability was measured using 3-[4,5-dimethylthiazol-2-yl]-2,5-diphenyltetrazoliumbromide (MTT) assay as previously described (17). Briefly, cells were cultured in complete medium in 48-well plates ($1 \times 10^4$ cells/well) for 48 hours and then treated in 10% FBS medium for 24, 48, or 72 hours. Fresh MTT (Sigma), resuspended in PBS, was then added to each well (final concentration 0.33 mg/mL). After 2-hour incubation, cells were lysed with 200 μL of DMSO, and optical density was measured at 570 nm in a multiplate reader (Synergy H1, BioTek, Agilent).

### Intracellular cholesterol extraction and colorimetric cholesterol assay

Cholesterol was measured using a colorimetric cholesterol assay kit (Cell Biolabs). Intracellular cholesterol was extracted from cells using a mixture of chloroform, isopropanol, and NP-40 (7: 11: 0.1). The same mix was added to tumor samples of known weight, and lysed using stainless steel beads in the Bullet Blender Tissue Homogenizer (Next Advance, Inc.). Purified water was then added to lysed samples, and upon centrifugation, the organic, bottom phase was taken and dried by vacuum centrifugation. The resulting lipid pellet was resuspended in 200 μL of 1X cholesterol assay buffer. Then, 50 μL of sample was processed according to the manufacturer's instruction.

### ELISA for estradiol

The H295R cells were kept in complete medium for 48 hours in multiwells of 12 ($1 \times 10^5$ cells/well) and treated in DMEM F-12 enriched with 5% DCC-FBS (FBS treated with Dextran coated in order to repair steroids) with increasing doses of simvastatin (2.5, 5, and 10 μmol/L). After 48 hours of treatment, the contents of 17β-estradiol (E2) were measured by means of ELISA (NovaTec) following the manufacturer's instruction.

### Spheroids culture

A single-cell suspension was prepared using enzymatic (1X Trypsin-EDTA, Sigma Aldrich, #T3924) and manual disaggregation (25-gauge needle; ref. 18). Cells were plated at a density of 500 cells/cm$^2$ in spheroids medium [DMEM-F12/B27/EGF (20 ng/mL)/Pen-Strep] in nonadherent conditions, in culture dishes coated with (2-hydroxyethylmethacrylate; poly-HEMA, Sigma, #P3932). Cells were grown for 5 days and maintained in a humidified incubator at 37°C at an atmospheric pressure in 5% (v/v) carbon dioxide/air. After 5 days of culture, spheres >50 μm were counted using an eye piece graticule, and the percentage of cells plated which formed spheres was calculated and is referred to as percentage spheroids formation, and was normalized to one (1 = 100% TSFE, tumor-spheres formation efficiency). Cells were directly seeded on low-attachment plates in the presence of treatments.

### Colony formation

The NCI-H295R cells were plated in 12-well plates ($1 \times 10^3$) and allowed to attach. Treatment commenced for 24 hours with drug alone. Untreated or simvastatin-treated cells were controls. The medium was changed, and surviving cells were allowed to grow colonies of ≥50 cells for 2 weeks, washed, fixed, stained with Coomassie blue, and counted. Total colony numbers were normalized to untreated controls.

### Protein extraction and Western blotting

H295R cells were cultured in complete medium for 48 hours in 100 mm plates ($2 \times 10^6$ cells) before being treated in complete medium with simvastatin for 48 hours and then used for cytosolic and mitochondrial protein extraction. The extracts were then analyzed by Western blotting (WB).

Total proteins were prepared using RIPA buffer. Equal amounts of proteins were subjected to WB analysis. Blots were incubated overnight at 4°C with primary antibodies. Membranes were incubated with horseradish peroxidase (HRP)–conjugated secondary antibodies (Amersham), and immunoreactive bands were visualized with the ECL (Amersham).

### Xenograft experiments

All animal procedures approved by the Ethics Research Committee University animals from Calabria (protocol no. 1077/2016-PR from the Ministry of Health to Dr. Sirianni) were performed in female Foxn1nu mice (Harlen Envigo) mice. Following H295R xenograft establishment, mice received 4 mg/kg/d of simvastatin in the water for

24 days, and tumors were harvested and weighed. The water with the treatment has been replaced every week. The dose was chosen to equal the therapeutic dose used for patients of 20 mg/d (based on the equivalence of body surface area; ref. 19).

### Immunohistochemistry

IHC experiments were performed using 8-mm-thick paraffin-embedded sections of H295R xenograft tumors from mice treated with vehicle or simvastatin. Slides were deparaffinized and dehydrated and incubated overnight at 4°C with Aromatase (MBL International Corporation, MCA2077S, 1:50), COXIV (Abcam, ab14744, 1:200), Ki-67 (DAKO, M7240, 1:100), CCNE (Bethyl, IHC-00341, 1:100), ERα (Santa Cruz Biotechnology, sc-8002, 1:50), and TOM20 (Santa Cruz Biotechnology, sc-17764, 1:100) primary antibodies. Then, a horse biotinylated anti-mouse/rabbit IgG was applied for 1 hour at room temperature (RT), to form the avidin biotin HRP complex (Vector Laboratories). Immunoreactivity was visualized by DAB (Vector Laboratories). For ERα detection, FITC-conjugated secondary antibodies (Santa Cruz Biotechnology) were used for 1 hour at RT. Fluorescent images were collected on Olympus fluorescent microscope.

### Oil red O staining

H295R cells ($1 \times 10^6$) were plated on glass coverslips for 48 hours and then treated for 48 hours with simvastatin (10 μmol/L). The cells were washed with cold PBS and fixed with 4% paraformaldehyde for 30 minutes at RT. Then, the cells were stained with 0.5% Oil Red O (Sigma-Aldrich) solution for 20 minutes at RT and counterstained with hematoxylin for 2 minutes, followed by PBS washes and microscopic evaluation.

### Cytochrome C oxidase/complex IV activity

Cryostat sections (8 μm) were prepared and stored at −80°C until use. For the cytochrome C oxidase (COX) activity staining, frozen sections were brought to RT, washed for 5 minutes with 25 mmol/L sodium phosphate buffer, pH 7.4, and then incubated for 0.5, 1, or 2 hours at 37°C with the COX incubation mixture. The COX solution consisted of 10 mg Cytochrome C (cat# C7752, Sigma-Aldrich), 10 mg 3,3′-diaminobenzidine tetrahydrochloride hydrate (cat# D5637, Sigma-Aldrich), and 2 mg catalase (cat# C1345, Sigma-Aldrich) dissolved in 10 mL of 25 mmol/L sodium phosphate buffer. The solution was filtered after preparation, and the pH was adjusted to 7.2 to 7.4 with 1 N NaOH.

### HMGCR activity assay

The HMGCR activity in H295R lysates was measured with HMGCR Activity Assay Kit (CS1090, Sigma) according to the manufacturer's instructions. The assay is based on the spectrophotometric measurement of the decrease in absorbance at 340 nm, which represents the oxidation of NADPH by the catalytic subunit of HMGCR in the presence of the substrate HMG-CoA. Cells were lysed in RIPA buffer containing protease inhibitors. Two microliters of cell lysate were used to measure HMGCR activity. One unit converts 1.0 μmol of NADPH to NADP+ per 1 minute at 37°C. The unit-specific activity is defined as μmol/min/mg protein (units/mg P).

### Detection of apoptosis by terminal deoxynucleotidyl transferase dUTP nick end labeling assay

The induction of apoptosis was assessed by the terminal deoxynucleotidyl transferase dUTP nick end labeling (TUNEL) assay, a method that evaluates the fragmentation of DNA. The click-it TUNEL Alexa Fluor Imaging Assay kit (Invitrogen) was used following the manufacturer's instructions. Sections of vehicle- and simvastatin-treated tumors from paraffin-embedded H295R xenografts were cut to a thickness of 5 μm, deparaffinized, dehydrated, and then used for the assay.

### Seahorse XFe96 metabolic flux analysis

Real-time oxygen consumption rates (OCR) for H295R cells treated with simvastatin or vehicle (control) were determined using the Seahorse Extracellular Flux (XF96) analyzer (Seahorse Bioscience). H295R cells were maintained in DMEM supplemented with 10% FBS, 2 mmol/L GlutaMAX, and 1% Pen/Strep. Note that $7 \times 10^4$ cells were seeded per well into XF96-well cell culture plates (Seahorse Bioscience) and incubated overnight at 37°C in a 5% $CO_2$ humidified atmosphere. After 24 hours, cells were treated with simvastatin (2.5, 5, and 10 μmol/L) for 48 hours. At the end of treatment, cells were processed as previously published (20).

### Microarray

H295R cells ($1 \times 10^5$) were plated on 60-mm dishes for 48 hours and then treated for 24 hours with Mitotane (25 μmol/L). RNA was extracted using PureLink RNA Mini Kit (Thermo Fisher). The quality of total RNA was first assessed using an Agilent Bioanalyzer 2100 (Agilent Technologies). Biotin-labeled cDNA targets were synthesized starting from 150 ng of total RNA. Double-stranded cDNA synthesis and related cRNA were performed with GeneChip WT Plus Kit (Affymetrix). The same Kit was used to synthesize the sense strand cDNA before to be fragmented and labeled. All steps of the labeling protocol were performed as suggested by Affymetrix, starting from 5.5 μg of ssDNA. Hybridization was performed using the GeneChip Hybridization, Wash, and Stain Kit. A single GeneChip Clariom S was then hybridized with each biotin-labeled sense target. GeneChip arrays were scanned using an Affymetrix GeneChip Scanner 3000 7G using default parameters. Affymetrix GeneChip Command Console software (AGCC) was used to acquire GeneChip images and generate . DAT and CEL files, which were used for subsequent analysis with proprietary software.

### RNA extraction, reverse transcription, and real-time PCR

Following total RNA extraction, 1 μg of total RNA was reverse transcribed and then used for PCR reactions performed in the iCycler iQ Detection System (Bio-Rad Laboratories S.r.l.). Final results were expressed as n-fold differences in gene expression relative to 18S and calibrator, calculated using the ΔΔCt method as previously shown (14).

### Patients' data analysis

Gene expression and survival data were obtained using two independent cohorts of adrenocortical tumors as follows: Expression Cohort included 33 ACC, 22 adrenocortical adenoma (ACA), and 10 normal adrenal (NC; GEO dataset GSE33371) and The Cancer Genome Atlas cohort included 78 ACC (https://portal.gdc.cancer.gov/legacy-archive).

### Statistical analysis

All experiments were performed at least 3 times. Data were expressed as mean values + standard error, and statistical significance between control and treated samples was analyzed using GraphPad Prism 5.0 (GraphPad Software, Inc.) software. Control and treated groups were compared using *t* test or the ANOVA. Significance was defined as $P < 0.05$. Microarray data analysis was performed using Partek Genomics Suite software (PGS), version 6.6 (6.16.0812 for

Mac). Affymetrix CEL-files were extracted, normalized, and summarized using RMA algorithm (CEL file imported by Partek on Wed Feb 21 10:25:17 2018; Probes to Import: Interrogating Probes; Probe filtering: skip; Algorithm: RMA; Background Correction: RMA Background Correction; Normalization: Quantile Normalization; Log Probes using Base: 2; Probeset Summarization: Median Polish; refs. 21–23). Genes differentially expressed were identified using a *t* test.

## Results

### Mitotane increases intratumor cholesterol content by affecting expression of genes involved in the regulation of cholesterol homeostasis

Here, we wanted to determine if mitotane can also increase cholesterol content in the tumor. As it can be seen in **Fig. 1A**, cholesterol is increased in ACC from patients treated with mitotane compared with tumors from patients with ACC that underwent surgery prior to any treatment. A key enzyme in cholesterol synthesis is HMGCoA reductase (HMGCR). We conducted a retrospective analysis of publicly available microarray data from cohorts of patients with ACC. Expression levels of *HMGCR* are higher in ACC when compared with the NC (**Fig. 1B**). However, its expression does not affect patients' survival (**Fig. 1C**). We evaluated HMGCR protein expression and activity in H295R cells after 2 and 14 days of mitotane treatment. Mitotane increases the enzyme activity (**Fig. 1D**) as previously demonstrated in hepatocytes (**Fig. 1D**).

We also used H295R cells treated with mitotane for 24 hours to perform gene expression microarray analysis. Using a cutoff of 1.5 in fold change and a $P$ value $\leq 0.05$, we identified 344 transcripts regulated by mitotane. Importantly, an enrichment analysis for the categories of Gene Ontology (GO) indicated that the drug preferentially increases expression of genes involved in metabolism, and more specifically, we looked into cholesterol metabolism (**Fig. 1E**). Among the genes present in this GO group, we further investigated sterol regulatory element-binding protein 1 (*SREBP1*) and insulin-induced gene 1 (*INSIG1*) encoding for proteins working as cholesterol sensors, and ATP-binding cassette subfamily G member 1 (*ABCG1*), encoding for a protein that mediates cholesterol efflux from the cells to ApoA1 (apolipoprotein A1), a component of HDL. Results from microarray were confirmed by real-time PCR using short-term (24 hours) and long-term (2 and 3 weeks) mitotane-treated H295R cells. As observed in microarray data, *SREBP1, INSIG1*, and *ABCG1* expression was decreased after 24-hour treatment (**Fig. 1F**, **I**, and **L**). On the long-term treatment, expression of SREBP1 was maintained at low level (**Fig. 1G**). Survival data for this factor show that when its expression is low, patients have a trend to a worse outcome, even if not significant (**Fig. 1H**). For INSIG1 and ABCG1, we found that long-term treatment with mitotane did not produce a decrease in gene expression, but mRNA levels were kept similar to those seen in untreated samples (**Fig. 1J** and **M**). The higher expression of these genes maintained in the presence of increased cholesterol amounts (caused by mitotane) indicates loss of cell ability to sense cholesterol levels. Importantly, survival data for *INSIG1* indicate that higher expression is associated with worse survival (**Fig. 1K**). A similar trend in the association was observed for *ABCG1*, even if there was not a significant difference between the two groups (**Fig. 1N**).

### A decrease in ACC intracellular cholesterol positively associates with decreased tumor growth *in vitro* and *in vivo*

The use of simvastatin was able to reduce H295R cell viability in a time- and dose-dependent manner (**Fig. 2A**). Importantly, the decreased cell viability was rescued by addition of mevalonate, the product of HMGCoA reductase activity (**Fig. 2B**). These effects were reproduced by fluvastatin and rosuvastatin (Supplementary Fig. S1A). In addition, we used two additional cell lines, SW13 and Y1, and found that all tested statins produced effects similar to those observed in H295R cells (Supplementary Fig. S1B and S1C). In the clonogenic assay, simvastatin-treated cells formed significantly less colonies when compared with vehicle-treated cells, illustrating the tumor-suppressor function of this drug (**Fig. 2C**). When H295R cells were grown as spheroids in the presence of simvastatin, we observed a substantial dose-dependent decrease in sphere numbers (**Fig. 2D**). To evaluate if intratumor cholesterol depletion could reduce ACC growth *in vivo*, xenografts were generated by implanting H295R cells in the flank of athymic nude mice. When tumors reached an average of 200 $mm^3$, mice were administered vehicle versus simvastatin at 4 mg/kg/day for 24 days, and tumors were measured twice a week. Tumor growth of the statin-treated group was significantly smaller than the vehicle-treated group (**Fig. 2E**). Tumor volume at the end of the experiment was 60% smaller in animals receiving simvastatin (**Fig. 2E**), and tumor weight was decreased by 58% (**Fig. 2F**). In parallel with the decline in tumor size with simvastatin, there was a decrease in Ki-67 staining (**Fig. 2G**; Supplementary Fig. S2A).

### Decreased cholesterol availability in ACC impairs estradiol production

After 48-hour treatment, simvastatin at the dose of 10 μmol/L caused a 33% reduction in intracellular cholesterol (**Fig. 3A**). We also evaluated cholesterol content in of H295R xenografts. By adjusting to tissue weight, we found a concentration of 9 ng/mg of tissue, whereas statin decreased this amount to 6.3 ng/mg of tissue (**Fig. 3B**). In addition, frozen sections from tumors were stained for lipids using Oil Red O, and less red stain is observed in treated tumors, indicative of a reduced amount of lipid deposition (**Fig. 3B**; Supplementary Fig. S2B). Thus, intratumor cholesterol has an important cell-autonomous role in ACC growth and in parallel statins lessens ACC tumor development. Treatment of H295R cells for 48 hours with increasing concentrations of simvastatin decreased E2 production in a dose-dependent manner, as demonstrated by ELISA of H295R culture media, with 10 μmol/L producing a 50% decrease in E2 content (**Fig. 3C**). When we evaluated aromatase (*CYP19*) gene expression, we did not find any change in mRNA, neither *in vitro* (**Fig. 3D**) nor *in vivo* (**Fig. 3G**), indicating that simvastatin does not affect transcriptional regulation of this gene. In fact, expression of steroidogenic factor 1 (SF-1) did not change after simvastatin treatment (**Fig. 3E**). However, WB analysis indicated a decrease in aromatase protein content following statin treatment of H295R (**Fig. 3F**), data that were confirmed by IHC on xenografts tumors (**Fig. 3H**; Supplementary Fig. S2C). In addition, the presence of mevalonate was able to overcome the inhibition on aromatase expression seen in the presence of simvastatin (Supplementary Fig. S3A).

### Decreased E2 availability in ACC impairs ERα function

ERα has a role in regulating transcription of mitochondrial genes involved in cellular respiration (24). We evaluated both nuclear and mitochondrial ERα activities after simvastatin treatment. Expression of ERα was decreased by simvastatin *in vitro* (**Fig. 4A**; Supplementary Fig. S4A and S4B) and *in vivo* (**Fig. 4B**; Supplementary Fig. S2D), and a similar effect was observed on cyclin E, a known target of ERα, both *in vitro* and *in vivo* (**Fig. 4C** and **D**; Supplementary Fig. S2E). In addition, the presence of mevalonate was able to overcome the

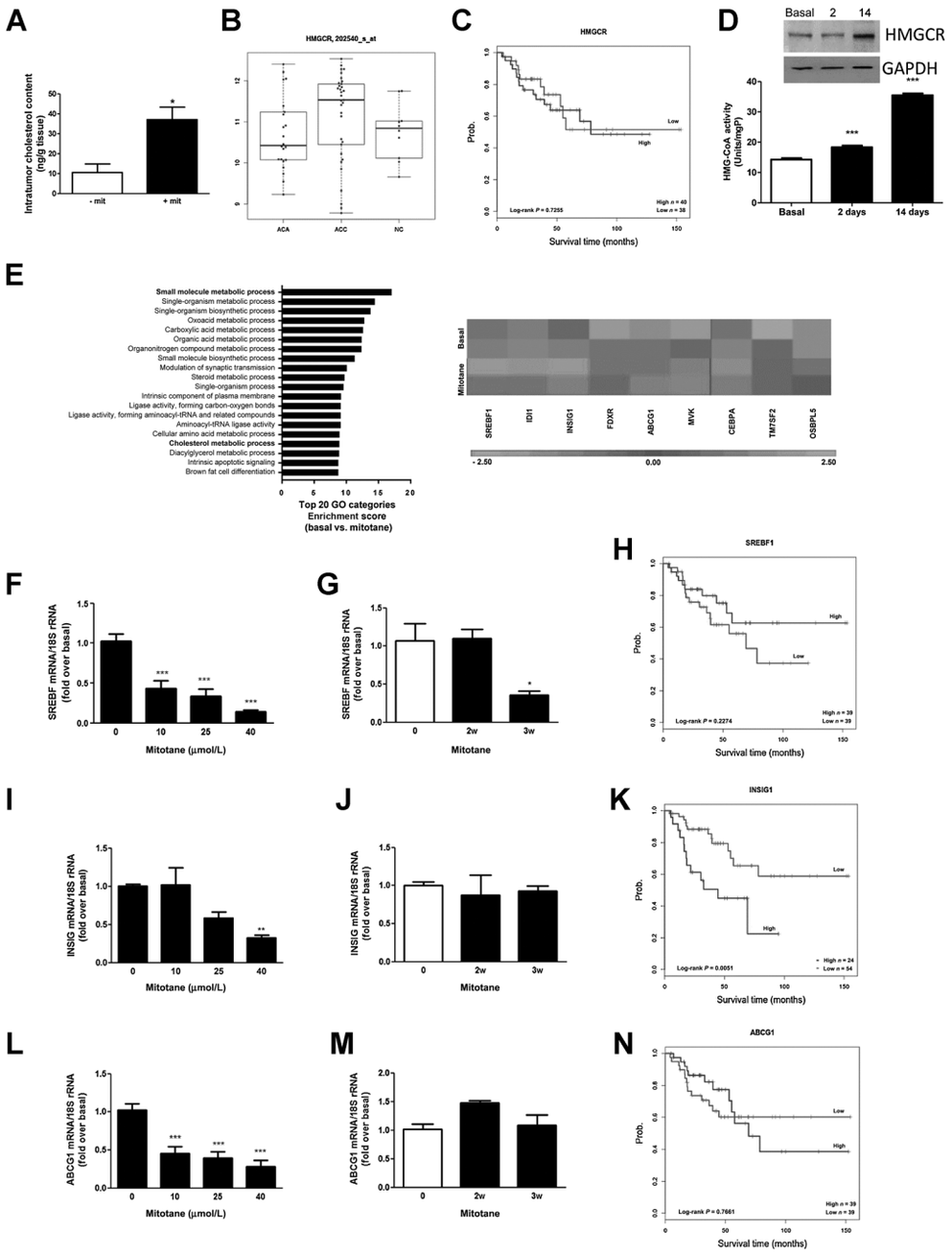


**Figure 1.**

Mitotane changes the expression of genes involved in cholesterol homeostasis in ACC and negatively affects patients' survival. **A,** Cholesterol was extracted from human ACC samples and its content (ng/mg tissue) measured by colorimetric assay (− Mitotane, $n = 5$, + Mitotane, $n = 7$; *, $P < 0.03$). **B,** Box plot graph for HMGCR gene expression in ACA, ACC, and NC human samples. ACC-ACA: $P$ value = 0.08, ACA-NC: $P$ value = 0.26, ACC-NC: $P$ value = 0.26. Statistical significance was calculated using *limma*. **C,** Survival time in patients with ACC according to *HMGCR* gene expression. **D,** HMGCR expression and activity were evaluated in H295R cells untreated (basal) or treated for 2 and 14 days with mitotane (10 µmol/L). **E,** RNA from H295R cells left untreated (basal) or treated for 24 hours with mitotane (25 µmol/L) was processed for microarray analysis. Enrichment analysis for the categories GO and heat map from microarray data with the most highly upregulated (red) and downregulated (blue) genes involved in the cholesterol biosynthesis pathway. **F** and **G, I** and **J, L** and **M,** mRNA expression of *SRBP1* (**F** and **G**), *INSIG1* (**I** and **J**), and *ABCG1* (**L** and **M**) in H295R cells. The mRNA was extracted and analyzed by QPCR from cells left untreated (0) or treated for 24 hours with Mitotane (10–25–40 µmol/L; **F**, **I**, and **L**) and from cells untreated (0) or treated for different weeks (2 or 3 weeks, w) with Mitotane (10 µmol/L; **G**, **J**, and **M**). Each sample was normalized to 18S rRNA content. Final results are expressed as n-fold differences of gene expression relative to calibrator. Data represent the mean ±SD of values from at least three separate RNA samples (*, $P < 0.05$ and ***, $P < 0.001$ versus calibrator). **H**, **K**, and **N,** Survival time in patients with ACC according to the expression of *SREBP1* (**H**), *INSIG1* (**K**), and *ABCG1* (**N**) genes. Statistical significance was calculated using $t$ test (**A–C**, **H**, **K**, and **N**) or one-way ANOVA followed by a Tukey *post-hoc* multiple comparison test (**D**, **F** and **G**, **I** and **J**, and **L** and **M**). $P < 0.05$ was considered significant.

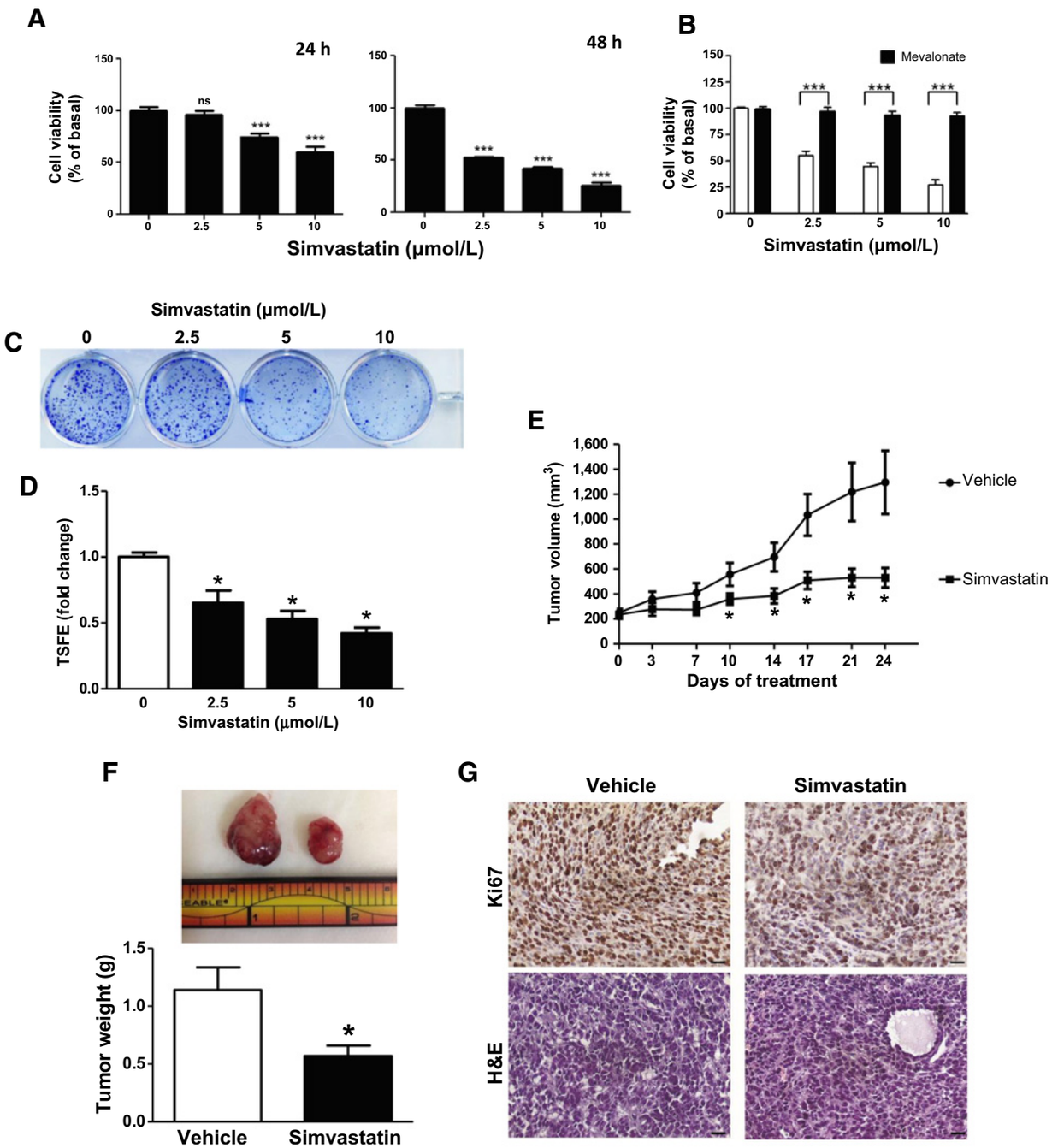


**Figure 2.**

Simvastatin reduces H295R cell growth, *in vitro* and *in vivo*. **A,** H295R cells were left untreated (0) or treated with increasing doses (2.5, 5, and 10 μmol/L) of simvastatin for 24 and 48 hours. **B,** H295R cells were left untreated (0) or treated with increasing doses (2.5, 5, and 10 μmol/L) of simvastatin with or without mevalonate (100 μmol/L) for 48 hours. **A** and **B,** Cell viability was evaluated by MTT assay (*, $P < 0.05$ and ***, $P < 0.001$ vs. 0). **C,** Representative image of colony formation assay performed on H295R cells (1,000 cells/well) plated for 2 weeks in the presence of simvastatin (2.5, 5, and 10 μmol/L). **D,** H295R cells were plated on low-attachment plates and then left untreated (0) or treated with Simvastatin (2.5, 5, and 10 μmol/L), and TSFE was evaluated 5 days later (*, $P < 0.05$ vs. untreated cells). **E,** H295R cells were injected subcutaneously in the flank region of nude mice, and the resulting tumors were grown to an average of 200 $mm^3$ 21 days after inoculation and then treated with vehicle ($n = 8$) or simvastatin ($n = 7$; 4 mg/kg/day) for 24 days. Values represent the mean ±SE of measured tumor volume over time (*, $P < 0.05$ vs. control). **F,** Representative tumors and final tumor weights, and values are mean ±SEM (*, $P < 0.05$ vs. vehicle). **G,** Ki67 IHC and hematoxylin and eosin (H&E) staining of H295R xenografts (magnification, ×20; scale bar, 25 μm). Statistical significance was calculated using *t* test (**F**) or one-way ANOVA followed by a Tukey *post-hoc* multiple comparison test (**A**, **B**, **D**, and **E**). $P < 0.05$ was considered significant.

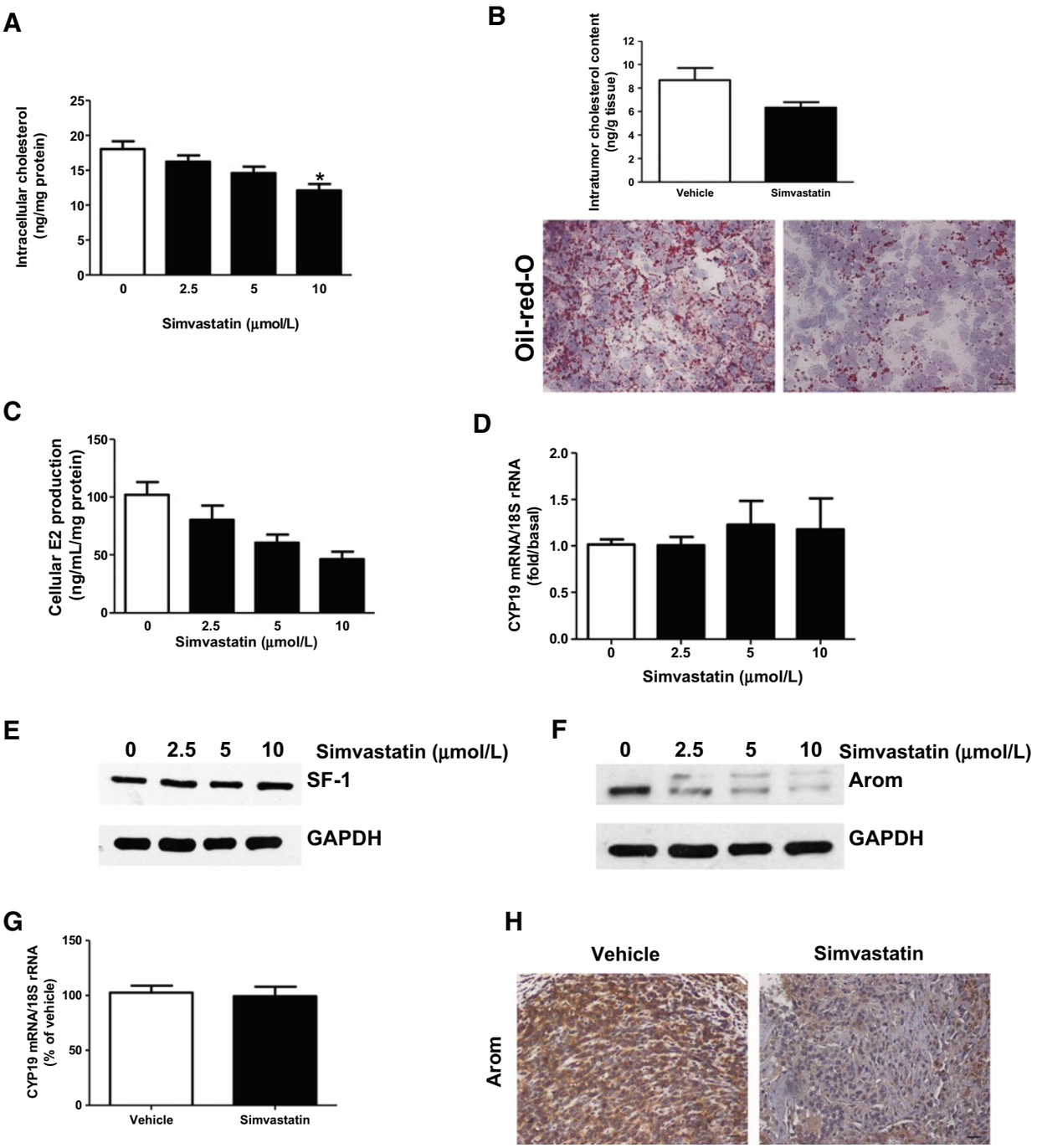


**Figure 3.**

Simvastatin decreases cholesterol and aromatase content in ACC. **A,** H295R cells were left untreated (0) or treated for 48 hours with simvastatin (2.5, 5, and 10 μmol/L) in growth medium containing 10% lipoprotein-free serum. Cholesterol was extracted and measured by colorimetric assay (*, $P < 0.05$ vs. untreated cells). **B,** (bar graph) Cholesterol content in H295R xenografts samples (*, $P < 0.05$ vs. vehicle; $n = 8$ vehicle; $n = 7$ Simvastatin). **B,** (photograph) Frozen sections of H295R xenografts from vehicle- or simvastatin-treated mice were used for lipids droplets staining by Oil Red O (magnification, ×40; scale bar, 12.5 μm). **C,** H295R cells were treated for 48 hours with the indicated doses of simvastatin added to 5% DCC-FBS, and estradiol (E2) release in the culture medium was measured by ELISA. Values represent the mean ± SE (*, $P < 0.05$ vs. untreated cells). **D–F,** H295R cells untreated (0) or treated for 24 hours with simvastatin (2.5, 5, and 10 μmol/L) were analyzed for *CYP19* gene expression normalized to 18S rRNA by real-time PCR (**D**), and for SF-1 (**E**) or Aromatase (Arom, **F**) protein content by WB. GAPDH was used as a loading control. Blots are from first representative experiment out of at least three performed. **G,** *CYP19* expression in H295R xenografts' samples from vehicle- or simvastatin-treated mice by real-time PCR ($n = 8$ vehicle; $n = 7$ Simvastatin). **H,** IHC staining of Aromatase in untreated or simvastatin-treated H295R xenograft samples (magnification, ×20; scale bar, 25 μmol/L). Statistical significance was calculated using *t* test (**B** and **G**) or one-way ANOVA followed by a Tukey *post-hoc* multiple comparison test (**A**, **C**, and **D**). $P < 0.05$ was considered significant.

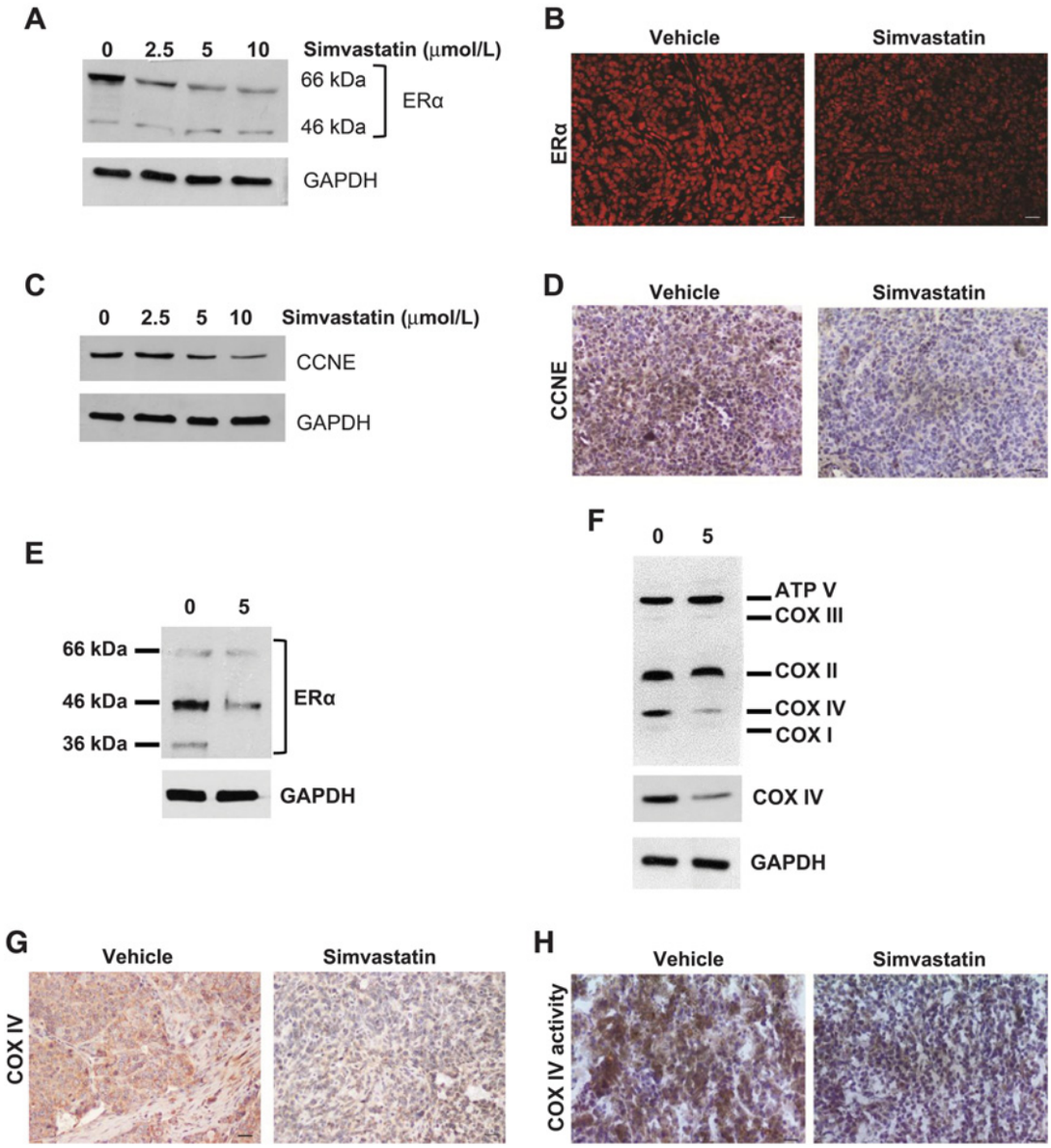


**Figure 4.**

Simvastatin reduces nuclear and mitochondrial ERα activity. **A** and **C,** WB analysis of ERα (**A**) and Cyclin E (**C**) was performed on equal amounts of total protein extracts from H295R cells left untreated (0) or treated with Simvastatin (2.5, 5, and 10 μmol/L) for 48 hours. GAPDH was used as a loading control. Blots are representative of three independent experiments with similar results. **B** and **D,** Immunofluorescence analysis of ERα expression (**B**) and IHC staining of Cyclin E (**D**) on H295R xenograft tumor samples obtained from vehicle- or simvastatin-treated mice (magnification, ×20; scale bar, 25 μmol/L). **E** and **F,** H295R cells untreated (0) or treated with simvastatin (5 μmol/L) were used for mitochondrial protein extraction. ERα (**E**) and OXPHOS (**F**) protein expression was analyzed by WB. GAPDH was used as a loading control. Blots are representative of three independent experiments with similar results. **G** and **H,** Immunostaining (**G**) and activity (**H**) of COXIV were evaluated on H295R xenograft samples obtained from vehicle- or simvastatin-treated mice (magnification, ×20; scale bar, 25 μm).

inhibition on ERα expression seen in the presence of simvastatin (Supplementary Fig. S3A).

These effects are opposite to those elicited by E2, which instead increased cyclin E expression (Supplementary Fig. S3B). Mitochondrial protein fraction was used for WB analysis of ERα, and we observed that simvastatin-treated samples had a lower content of the nuclear receptor (**Fig. 4E**). WB analysis of all the components of the respiratory chain (COX I to IV plus ATP synthase) can be performed using a mix of five different antibodies (OX-PHOS). With this approach, we identified a decreased expression of COXIV (**Fig. 4F**; Supplementary Fig. S4A and S4B), a known target of ERα. On the contrary, E2 treatment increased COXIV expression and is able to prevent statin-inhibitory effect (Supplementary Fig. S3C). Data were also confirmed on statin-treated xenografts where we observed a reduced COXIV expression (**Fig. 4G**; Supplementary Fig. S2F) and activity (**Fig. 4H**; Supplementary Fig. S2G) compared with vehicle-

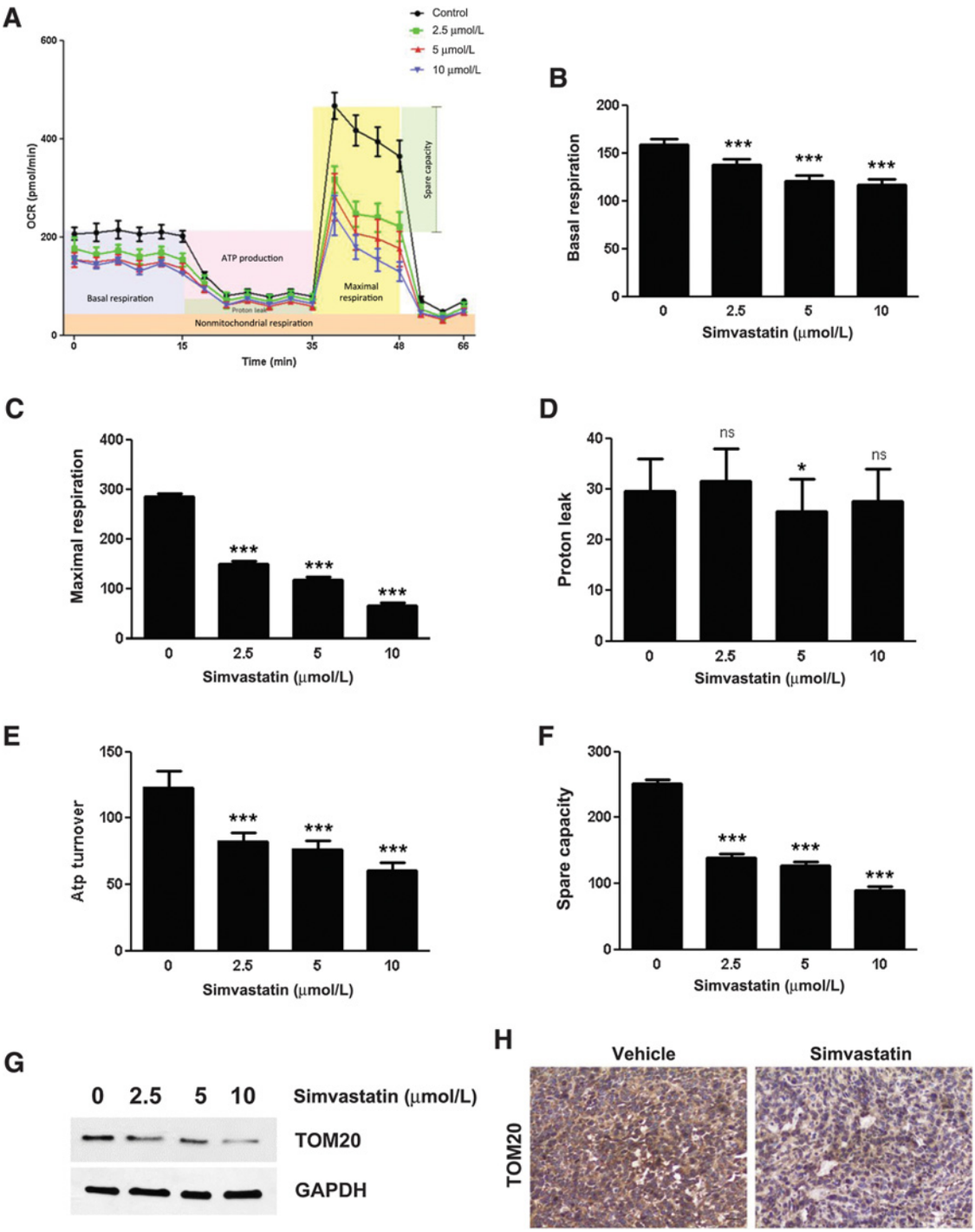


**Figure 5.**

Simvastatin reduces mitochondrial functions. **A–F,** Mitochondrial respiration described as OCR levels was detected in H295R cells left untreated or treated with Simvastatin (2.5, 5, and 10 μmol/L) for 16 hours by Seahorse XFe96 analyzer. **A,** The linear graph shows time course measurements but with three different injections to evaluate the OCR (1) after the oligomycin injection, (2) after the injection of carbonyl cyanide-(trifuoromethoxy)phenylhydrazone (FCCP), and (3) after the injection of rotenone/antimycin. **B–F,** The histograms are derived from the obtained measurements: (**B**) basal respiration, (**C**) maximal respiration, (**D**) proton leak, (**E**) ATP turnover, and (**F**) spare capacity (*, $P < 0.05$ and ***, $P < 0.001$ simvastatin vs. untreated cells). **G,** Mitochondrial extracts from H295R cells treated for 48 hours were analyzed for TOM20 protein expression by WB. **H,** TOM20 protein expression was evaluated by IHC on H295R xenograft samples obtained from vehicle- or simvastatin-treated mice (magnification, ×20; scale bar, 25 μm).

treated xenografts. We monitored cellular OCR and demonstrated that simvastatin is able to reduce oxygen consumption in a dose-dependent manner (**Fig. 5A**). Statin exposure profoundly affected the oxidative metabolism of H295R cells. Indeed, 16 hours of treatment induced a clear dose-dependent decrease of the basal (**Fig. 5B**) and maximal respiration (**Fig. 5C**) as well as ATP turnover (**Fig. 5E**) and spare capacity (**Fig. 5F**). No effect was observed on proton leak (**Fig. 5D**). We also used immunoblotting to monitor the abundance of a known reliable marker of mitochondrial mass, TOM20, in response to simvastatin treatment. We found that treated H295R cells displayed a reduced expression of TOM20, *in vitro* and *in vivo* (**Fig. 5G** and **H**; Supplementary Fig. S2H).

### Decreased cholesterol availability in ACC activates an apoptotic pathway

BAK expression and PARP-1 cleavage were increased in H295R cells treated for 48 hours with simvastatin, indicating activation of apoptosis (**Fig. 6A**; Supplementary Fig. S4C and S4D), further confirmed by TUNEL assay (**Fig. 6B**). Similarly, evaluation of apoptosis on H295R xenografts sections revealed an increase of TUNEL-positive cells under simvastatin treatment (**Fig. 6C**). Because Bak gene is under c-Jun transcriptional control (25), we evaluated c-Jun protein levels after simvastatin treatment. After 48 hours, we observed increased levels of c-Jun and its phosphorylation status, as well as increased levels of pERK1/2, whose sustained activation is associated with apoptosis (26). Addition of mevalonate prevented activation of these kinases in response to simvastatin (**Fig. 6D**; Supplementary Fig. S4C and S4D). Specific inhibitors for ERK1/2 and JNK abrogated Jun and ERK1/2 activation/phosphorylation preventing apoptosis, as indicated by the loss of PARP1 cleavage. These data indicate ERK1/2 and JNK as part of simvastatin-induced apoptotic mechanism (**Fig. 6E**). Similarly to simvastatin, fluvastatin and rosuvastatin inhibited estrogen signaling and activated apoptosis in H295R cells (Supplementary Fig. S4E and S4F).

## Discussion

Mitotane represents the first-line therapy for patients with ACC. However, mitotane alone or combined with chemotherapy shows limited efficacy on advanced disease. In addition, mitotane has high toxicity and several side effects including hypercholesterolemia (6, 27). Data from almost 40 years ago report the ability of mitotane to increase liver HMGCR activity *in vitro* and *in vivo* (5). Because the adrenal synthesizes cholesterol *de novo*, mitotane could have a direct effect on adrenal cholesterol synthesis. Having higher cholesterol bioavailability, tumor cells can foster their own growth. To support our hypothesis, we first demonstrate an increase in intratumor cholesterol in patients with ACC treated with mitotane compared with untreated patients. Using previously published microarray data publically available (28), we demonstrated the presence of increased HMGCR expression in ACC samples, which, however, was not associated with decreased survival rate. Increased intratumor cholesterol following mitotane treatment could be due to an increased activity of HMGCR rather than to an increased expression, with the former influencing survival more than the latter. Microarray analysis of mitotane-treated H295R cells helped us in identifying genes involved in cholesterol metabolism and modulated by the drug. Among them, we validated *INSIG1, SREBP1*, and *ABCG1*. *INSIG1* encodes for a protein that retains a chaperone protein (SCAP) in the endoplasmic reticulum, and SCAP is necessary for delivery of SREBP1 to the Golgi, where SREBP1 becomes active. SREBP1 increases transcription of cholesterol-synthesizing genes such as *HMGCR* (29).

Short-term mitotane decreases *INSIG1* and *SREBP1* expression, whereas long-term mitotane maintains low *SREBP1* but high *INSIG1* expression. When looking at survival data of patients with ACC, high *INSIG1* is associated with a shorter survival. *ABCG1* belongs to the family of ATP binding cassette and mediates cholesterol efflux (30). Its expression is decreased by short-term mitotane treatment, but this effect is lost after prolonged treatment, favoring cholesterol accumulation. Because mitotane has a prevalent accumulation in adipose tissue, the circulating levels are often reduced (13, 31), and the therapeutic concentrations of mitotane (between 14 and 20 μg/mL, 40 and 60 μmol/L) are not always reached in patients. Importantly, lower doses (10 and 25 μmol/L) produce effects that are different from what were seen using 40 μmol/L. This raises a question, could cells, in the presence of lower doses of mitotane, escape the normal control of cholesterol homeostasis? Can the increase in cholesterol be responsible for long-term adjustment to mitotane?

Several reports propose a promising role for statins in cancer treatment (32). Here, we demonstrate that simvastatin can reduce intratumor cholesterol synthesis. Based on MTT assay, $IC_{50}$ for simvastatin was calculated to be 10 μmol/L. Since 1 μmol/L simvastatin in the media corresponds to the dose of 0.4586 mg/kg of body weight, we decided to treat mice with 4 mg/kg/day. This dose is equivalent to a human dose of 20 mg/d based on body surface area equivalency. This dose was effective in producing more that 60% decrease in tumor growth. Importantly, this dose decreased intratumor cholesterol content, supporting our hypothesis that a reduction in intratumor cholesterol can decrease ACC growth. Interest for statins is not new for the therapy of ACC; however, it has been considered in association with mitotane to reduce hypercholesterolemia (6, 33). Our data instead suggest the possibility of using lipophilic statins without mitotane but eventually with cytotoxic drugs. Simvastatin, which appears to be the most effective among the tested drugs, should not be combined with mitotane, which is a known inducer of *CYP3A4*, a member of the cytochrome P450 family involved in simvastatin metabolism. A recent case study evaluated management of hypercholesterolemia induced by mitotane treatment. The use of statins, coadministred with mitotane, was uneffective in lowering cholesterol and LDL-c level. Importantly, the patient had two local recurrences within a 7-year period; however, the course of ACC in this patient's case has been better than average. These data support our hypothesis that cholesterol can be implicated in ACC progression.

Cholesterol in tumor adrenal cells is used for steroid synthesis, and a decrease in its availability would affect estradiol production. Our previous study demonstrated that E2 increases tumor growth, and Tamoxifen, which blocks ERα activity, prevents its effects (9). With this information as background, we wanted to investigate if the reduced E2 production, seen after simvastatin treatment, could interfere with ERα function. We first observed a reduction in CCNE, a known nuclear target of ERα. In addition, we investigated if the expression of mitochondrial targets of ERα could be influenced by simvastatin. To support a role for ERα in the mitochondria of tumor adrenal, we show that E2 treatment increases the amount of COXIV levels and prevents simvastatin-inhibitory effect.

In addition, direct effect of statins was reported on mitochondrial function, consequent to a deficiency of complex I (34). The novelty of our data is the involvement of ERα/complex IV in statin-mediated apoptosis. The reduction in COXIV alters the functioning of mitochondrial respiration, changing the mitochondrial potential ultimately

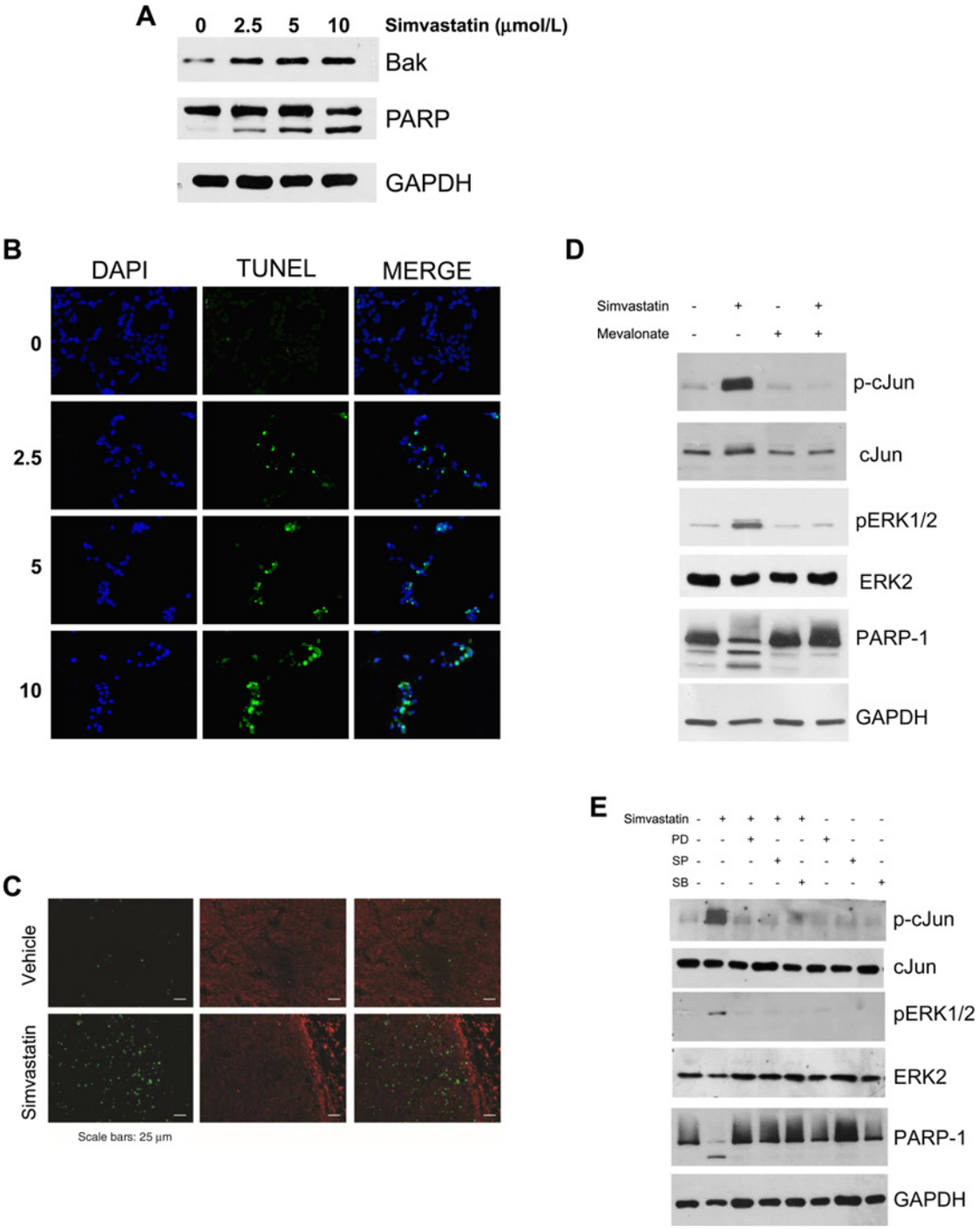


**Figure 6.**

*In vitro* and *in vivo* activation of apoptosis by simvastatin in ACC. **A,** Cells were left untreated (0) or treated with simvastatin (2.5, 5, and 10 μmol/L) for 48 hours. WB analyses of Bak and PARP-1 were performed on equal amounts of total protein extracts. GAPDH was used as a loading control. Blots are representative of three independent experiments with similar results. **B,** TUNEL assay was performed on cells treated as described in **A**. DAPI was used as nuclear counterstain. Fluorescent signal was observed under a fluorescent microscope. Images are from a representative experiment. **C,** TUNEL staining was performed on frozen sections of H295R xenograft samples obtained from vehicle- or simvastatin-treated mice (scale bar, 25 μm). **D,** WB analyses for p-cJun, c-Jun, pERK1/2, ERK2, and PARP-1 were performed on total protein extracted from cells treated for 48 hours with simvastatin (5 μmol/L), mevalonate (100 μmol/L), or their combination. **E,** WB analyses for p-cJun, Jun, pERK1/2, ERK2, and PARP-1 were performed on total protein extracted from cells treated for 48 hours with simvastatin (5 μmol/L) alone or combined with PD98059 (10 μmol/L), SP600125 (10 μmol/L), and SB203580 (10 μmol/L). GAPDH was used as a loading control.

leading to organelle damage. High COXIV activity within the tumor occurs in a significant subset of patients with high-grade gliomas and is an independent predictor of poor outcome (35). Importantly, it has been postulated that COXIV activity may be required for the anchorage-independent growth of lung cancer cells (36). In general, mitochondria appear to be an appealing target for the treatment of cancer (37). Effects on COXIV negatively influence mitochondrial function as demonstrated by reduced OCR. We have previously demonstrated that a reduced cell growth is observed in breast cancer cells treated with XCT790, a drug that targets ERRα, a master regulator of cell metabolism. ERRα inhibition reduces OCR and prevents tumor growth (20). We have also used XCT790 to block ERRα in ACC and demonstrated its efficacy in reducing tumor growth (38), further establishing that impairing mitochondrial function reduces ACC growth. It has been shown that mitotane significantly impairs mitochondrial respiratory chain function by selectively inhibiting enzymatic complex IV activity. However, as a consequence of respiratory chain inhibition, mitotane causes a compensatory increase of mitochondrial biogenesis (39). Differently from mitotane, simvastatin reduces TOM20, a marker of mitochondrial mass. Reduced mitochondrial function after treatment with simvastatin causes cell death by apoptosis, the same type of cell death that is observed in H295R and SW13 cells in response to mitotane. This apoptotic mechanism requires activation of c-Jun and sustained ERK1/2 phosphorylation. Farnesyl pyrophosphate or geranylgeranyl pyrophosphate are products of mevalonate that can be anchored onto intracellular proteins through prenylation, thereby ensuring the relocalization of the target proteins in the cell membranes (40–42). Ras is a prenylated protein upstream of ERK1/2 activation. The observation that ERK1/2 phosphorylation is maintained in the presence of simvastatin evidences that its phosphorylation is independent of Ras and potentially involves different pathways. We found that ERK phosphorylation is prevented by addition of p38 and JNK inhibitors, implicating these kinases in the observed sustained ERK activation. Jun expression and activation are increased by treatment with simvastatin and are reversed by addition of mevalonate, which also prevents PARP-1 cleavage, confirming that the apoptotic mechanism is dependent on cholesterol depletion.

Collectively, our data support the hypothesis of using statins for the treatment of ACC. Further preclinical studies are warranted to establish effects on tumor growth when used in combination with chemotherapy. However, their use in therapy as cholesterol-lowering drugs will easily translate preclinical studies into a clinical trial.

## Disclosure of Potential Conflicts of Interest

No potential conflicts of interest were disclosed.

## Authors' Contributions

**Conception and design:** V. Pezzi, I. Casaburi, R. Sirianni
**Development of methodology:** F. Trotta, P. Avena, A. Chimento, V. Rago, A. De Luca, S. Sculco, M.C. Nocito, F.M. Lasorsa, S.N. Barile, L. Palmieri, R. Sirianni
**Acquisition of data (provided animals, acquired and managed patients, provided facilities, etc.):** F. Trotta, R. Malivindi, R. Pezzani, R. Sirianni
**Analysis and interpretation of data (e.g., statistical analysis, biostatistics, computational analysis):** F. Fallo, C. Pilon, F.M. Lasorsa, S.N. Barile, L. Palmieri, A.M. Lerario, I. Casaburi, R. Sirianni
**Writing, review, and/or revision of the manuscript:** P. Avena, A. Chimento, I. Casaburi, R. Sirianni
**Administrative, technical, or material support (i.e., reporting or organizing data, constructing databases):** F. Trotta, A. De Luca
**Study supervision:** V. Pezzi, I. Casaburi, R. Sirianni

## Acknowledgments

This work was supported by Associazione Italiana per la Ricerca sul Cancro (AIRC) grant IG15230 to Dr. R. Sirianni and IG20122 to Dr. V. Pezzi. Drs. F. Trotta and P. Avena were supported by a fellowship from AIRC.

The costs of publication of this article were defrayed in part by the payment of page charges. This article must therefore be hereby marked *advertisement* in accordance with 18 U.S.C. Section 1734 solely to indicate this fact.

Received November 13, 2019; revised March 8, 2020; accepted June 11, 2020; published first June 16, 2020.

## References

1. Kirschner LS. The next generation of therapies for adrenocortical cancers. Trends Endocrinol Metab 2012;23:343–50.
2. Fassnacht M, Johanssen S, Quinkler M, Bucsky P, Willenberg HS, Beuschlein F, et al. Limited prognostic value of the 2004 international union against cancer staging classification for adrenocortical carcinoma: proposal for a revised TNM classification. Cancer 2009;115:243–50.
3. Hermsen IG, Fassnacht M, Terzolo M, Houterman S, den Hartigh J, Leboulleux S, et al. Plasma concentrations of o,p'DDD, o,p'DDA, and o,p'DDE as predictors of tumor response to mitotane in adrenocortical carcinoma: results of a retrospective ENS@T multicenter study. J Clin Endocrinol Metab 2011;96:1844–51.
4. Kerkhofs TM, Baudin E, Terzolo M, Allolio B, Chadarevian R, Mueller HH, et al. Comparison of two mitotane starting dose regimens in patients with advanced adrenocortical carcinoma. J Clin Endocrinol Metab 2013;98:4759–67.
5. Stacpoole PW, Varnado CE, Island DP. Stimulation of rat liver 3-hydroxy-3-methylglutaryl-coenzyme A reductase activity by o,p'-DDD. Biochem Pharmacol 1982;31:857–60.
6. Maher VM, Trainer PJ, Scoppola A, Anderson JV, Thompson GR, Besser GM. Possible mechanism and treatment of o,p'DDD-induced hypercholesterolaemia. Q J Med 1992;84:671–9.
7. Miller WL. Steroidogenesis: unanswered questions. Trends Endocrinol Metab 2017;28:771–93.
8. Barzon L, Masi G, Pacenti M, Trevisan M, Fallo F, Remo A, et al. Expression of aromatase and estrogen receptors in human adrenocortical tumors. Virchows Arch 2008;452:181–91.
9. Sirianni R, Zolea F, Chimento A, Ruggiero C, Cerquetti L, Fallo F, et al. Targeting estrogen receptor-alpha reduces adrenocortical cancer (ACC) cell growth in vitro and in vivo: potential therapeutic role of selective estrogen receptor modulators (SERMs) for ACC treatment. J Clin Endocrinol Metab 2012;97:E2238–50.
10. Miller BS, Ignatoski KM, Daignault S, Lindland C, Doherty M, Gauger PG, et al. Worsening central sarcopenia and increasing intra-abdominal fat correlate with decreased survival in patients with adrenocortical carcinoma. World J Surg 2012;36:1509–16.
11. Simpson ER. Sources of estrogen and their importance. J Steroid Biochem Mol Biol 2003;86:225–30.
12. Li J, Papadopoulos V, Vihma V. Steroid biosynthesis in adipose tissue. Steroids 2015;103:89–104.
13. Hescot S, Seck A, Guerin M, Cockenpot F, Huby T, Broutin S, et al. Lipoprotein-free mitotane exerts high cytotoxic activity in adrenocortical carcinoma. J Clin Endocrinol Metab 2015;100:2890–8.
14. Chimento A, Sirianni R, Casaburi I, Zolea F, Rizza P, Avena P, et al. GPER agonist G-1 decreases adrenocortical carcinoma (ACC) cell growth in vitro and in vivo. Oncotarget 2015;6:19190–203.
15. Weiss LM, Medeiros LJ, Vickery AL Jr. Pathologic features of prognostic significance in adrenocortical carcinoma. Am J Surg Pathol 1989;13:202–6.
16. Aubert S, Wacrenier A, Leroy X, Devos P, Carnaille B, Proye C, et al. Weiss system revisited: a clinicopathologic and immunohistochemical study of 49 adrenocortical tumors. Am J Surg Pathol 2002;26:1612–9.

17. De Luca A, Avena P, Sirianni R, Chimento A, Fallo F, Pilon C, et al. Role of scaffold protein proline-, glutamic acid-, and leucine-rich protein 1 (PELP1) in the modulation of adrenocortical cancer cell growth. Cells 2017;6:42.
18. Shaw FL, Harrison H, Spence K, Ablett MP, Simões BM, Farnie G, et al. A detailed mammosphere assay protocol for the quantification of breast stem cell activity. J Mammary Gland Biol Neoplasia 2012;17:111–7.
19. Reagan-Shaw S, Nihal M, Ahmad N. Dose translation from animal to human studies revisited. FASEB J 2008;22:659–61.
20. De Luca A, Fiorillo M, Peiris-Pages M, Ozsvari B, Smith DL, Sanchez-Alvarez R, et al. Mitochondrial biogenesis is required for the anchorage-independent survival and propagation of stem-like cancer cells. Oncotarget 2015;6:14777–95.
21. Bolstad BM, Irizarry RA, Astrand M, Speed TP. A comparison of normalization methods for high density oligonucleotide array data based on variance and bias. Bioinformatics 2003;19:185–93.
22. Irizarry RA, Bolstad BM, Collin F, Cope LM, Hobbs B, Speed TP. Summaries of Affymetrix GeneChip probe level data. Nucleic Acids Res 2003;31:e15.
23. Wu ZJ, Irizarry RA, Gentleman R, Martinez-Murillo F, Spencer F. A model-based background adjustment for oligonucleotide expression arrays. J Am Statist Assoc 2004;99:909–17.
24. Chen JQ, Cammarata PR, Baines CP, Yager JD. Regulation of mitochondrial respiratory chain biogenesis by estrogens/estrogen receptors and physiological, pathological and pharmacological implications. Biochim Biophys Acta 2009; 1793:1540–70.
25. Jin HO, Park IC, An S, Lee HC, Woo SH, Hong YJ, et al. Up-regulation of Bak and Bim via JNK downstream pathway in the response to nitric oxide in human glioblastoma cells. J Cell Physiol 2006;206:477–86.
26. Cagnol S, Chambard JC. ERK and cell death: mechanisms of ERK-induced cell death–apoptosis, autophagy and senescence. FEBS J 2010;277:2–21.
27. Daffara F, De Francia S, Reimondo G, Zaggia B, Aroasio E, Porpiglia F, et al. Prospective evaluation of mitotane toxicity in adrenocortical cancer patients treated adjuvantly. Endocr Relat Cancer 2008;15:1043–53.
28. Barlaskar FM, Spalding AC, Heaton JH, Kuick R, Kim AC, Thomas DG, et al. Preclinical targeting of the type I insulin-like growth factor receptor in adrenocortical carcinoma. J Clin Endocrinol Metab 2009;94:204–12.
29. Weber LW, Boll M, Stampfl A. Maintaining cholesterol homeostasis: sterol regulatory element-binding proteins. World J Gastroenterol 2004;10:3081–7.
30. Yvan-Charvet L, Wang N, Tall AR. Role of HDL, ABCA1, and ABCG1 transporters in cholesterol efflux and immune responses. Arterioscler Thromb Vasc Biol 2010;30:139–43.
31. van Slooten H, Moolenaar AJ, van Seters AP, Smeenk D. The treatment of adrenocortical carcinoma with o,p'-DDD: prognostic implications of serum level monitoring. Eur J Cancer Clin Oncol 1984;20:47–53.
32. Zhong S, Zhang X, Chen L, Ma T, Tang J, Zhao J. Statin use and mortality in cancer patients: systematic review and meta-analysis of observational studies. Cancer Treat Rev 2015;41:554–67.
33. Tsakiridou ED, Liberopoulos E, Giotaki Z, Tigas S. Proprotein convertase subtilisin-kexin type 9 (PCSK9) inhibitor use in the management of resistant hypercholesterolemia induced by mitotane treatment for adrenocortical cancer. J Clin Lipidol 2018;12:826–9.
34. Sirvent P, Bordenave S, Vermaelen M, Roels B, Vassort G, Mercier J, et al. Simvastatin induces impairment in skeletal muscle while heart is protected. Biochem Biophys Res Commun 2005;338:1426–34.
35. Griguer CE, Cantor AB, Fathallah-Shaykh HM, Gillespie GY, Gordon AS, Markert JM, et al. Prognostic relevance of cytochrome C oxidase in primary glioblastoma multiforme. PLoS One 2013;8:e61035.
36. Telang S, Nelson KK, Siow DL, Yalcin A, Thornburg JM, Imbert-Fernandez Y, et al. Cytochrome c oxidase is activated by the oncoprotein Ras and is required for A549 lung adenocarcinoma growth. Mol Cancer 2012;11:60.
37. Ralph SJ, Neuzil J. Mitochondria as targets for cancer therapy. Mol Nutr Food Res 2009;53:9–28.
38. Casaburi I, Avena P, De Luca A, Chimento A, Sirianni R, Malivindi R, et al. Estrogen related receptor alpha (ERRalpha) a promising target for the therapy of adrenocortical carcinoma (ACC). Oncotarget 2015;6: 25135–48.
39. Hescot S, Slama A, Lombes A, Paci A, Remy H, Leboulleux S, et al. Mitotane alters mitochondrial respiratory chain activity by inducing cytochrome c oxidase defect in human adrenocortical cells. Endocr Relat Cancer 2013;20: 371–81.
40. Nishida S, Matsuoka H, Tsubaki M, Tanimori Y, Yanae M, Fujii Y, et al. Mevastatin induces apoptosis in HL60 cells dependently on decrease in phosphorylated ERK. Mol Cell Biochem 2005;269:109–14.
41. Yanae M, Tsubaki M, Satou T, Itoh T, Imano M, Yamazoe Y, et al. Statin-induced apoptosis via the suppression of ERK1/2 and Akt activation by inhibition of the geranylgeranyl-pyrophosphate biosynthesis in glioblastoma. J Exp Clin Cancer Res 2011;30:74.
42. Wu J, Wong WW, Khosravi F, Minden MD, Penn LZ. Blocking the Raf/MEK/ERK pathway sensitizes acute myelogenous leukemia cells to lovastatin-induced apoptosis. Cancer Res 2004;64:6461–8.